European Journal of Medicinal Chemistry 221 (2021) 113514

Contents lists available at ScienceDirect

European Journal of Medicinal Chemistry

journal homepage: http://www.elsevier.com/locate/ejmech

$PdCl_2$-catalyzed synthesis of a new class of isocoumarin derivatives containing aminosulfonyl / aminocarboxamide moiety: First identification of a isocoumarin based PDE4 inhibitor

B. Thirupataiah [a, b], Guntipally Mounika [a], Gangireddy Sujeevan Reddy [a, b], Jetta Sandeep Kumar [a, b], Kazi Amirul Hossain [a], Raghavender Medishetti [a, b], Snigdha Samarpita [c], Mahaboobkhan Rasool [c], Jayesh Mudgal [b], Jessy E. Mathew [b], Gautham G. Shenoy [b], C. Mallikarjuna Rao [b], Kiranam Chatti [a], Kishore V.L. Parsa [a], Manojit Pal [a, *]

[a] Dr. Reddy's Institute of Life Sciences, University of Hyderabad Campus, Gachibowli, Hyderabad, 500 046, India
[b] Manipal College of Pharmaceutical Sciences, Manipal Academy of Higher Education, Madhav Nagar, Manipal, 576 104, Karnataka, India
[c] Immunopathology Lab, School of Biosciences and Technology, Vellore Institute of Technology (VIT), Vellore, India

ARTICLE INFO

Article history:
Received 19 March 2021
Received in revised form
22 April 2021
Accepted 28 April 2021
Available online 6 May 2021

Keywords:
Isocoumarin
Pd-catalyst
PDE-4
Inflammation
Zebrafish

ABSTRACT

While anti-inflammatory properties of isocoumarins are known their PDE4 inhibitory potential was not explored previously. In our effort the non-PDE4 inhibitor isocoumarins were transformed into the promising inhibitors *via* introducing an aminosulfonyl/aminocarboxamide moiety to the C-3 benzene ring attached to the isocoumarin framework. This new class of isocoumarins were synthesized *via* a $PdCl_2$-catalyzed construction of the 4-allyl substituted 3-aryl isocoumarin ring starting from the appropriate 2-alkynyl benzamide derivative. Several compounds showed good inhibition of PDE4B *in vitro* and the SAR indicated superiority of aminosulfonamide moiety over aminocarboxamide in terms of PDE4B inhibition. Two compounds **3q** and **3u** with PDE4B $IC_{50} = 0.43 \pm 0.11$ and 0.54 ± 0.19 μM and ≥ 2-fold selectivity over PDE4D emerged as initial hits. The participation of aminosulfonamide moiety in PDE4B inhibition and the reason for selectivity though moderate shown by **3q** and **3u** was revealed by the *in silico* docking studies. In view of potential usefulness of moderately selective PDE4B inhibitors the compound **3u** (that showed PDE4 selectivity over other PDEs) was further evaluated in adjuvant induced arthritic rats. At an intraperitoneal dose of 30 mg/kg the compound showed a significant reduction in paw swelling (in a dose dependent manner), inflammation and pannus formation (in the knee joints) as well as pro-inflammatory gene expression/mRNA levels and increase in body weight. Moreover, besides its TNF-α inhibition and no significant toxicity in an MTT assay the compound did not show any adverse effects in a thorough toxicity studies e.g. teratogenicity, hepatotoxicity, cardiotoxicity and apoptosis in zebrafish. Thus, the isocoumarin **3u** emerged as a new, safe and moderately selective PDE4B inhibitor could be useful for inflammatory diseases possibly including COVID-19.

© 2021 Elsevier Masson SAS. All rights reserved.

1. Introduction

Isocoumarins represent one of the important class of naturally occurring aromatic lactones possessing numerous biological properties including anti-inflammatory activities [1]. For example, a highly substituted isocoumarin derivative i.e. paepalantine (**A**, Fig. 1) isolated from the capitula of paepalanthus bromelioides has shown intestinal anti-inflammatory activity in the trinitrobenzenesulphonic acid model of rat colitis [2] whereas activities of fluorinated isocoumarins as well as 3,4-dihydroisocoumarins against TPA (12-*O*-tetradecanoylphorbol-13-acetate)-induced inflammation in mice have been documented [3]. Besides, a dual inhibitor of 5-LOX (5-lipoxygenase) and PGE2 (prostaglandin E2) production was identified *via* screening of a series of 3-aryl isocoumarin derivatives in HeLa cells [4]. Indeed, a naturally occurring

* Corresponding author.
E-mail address: manojitpal@rediffmail.com (M. Pal).

https://doi.org/10.1016/j.ejmech.2021.113514
0223-5234/© 2021 Elsevier Masson SAS. All rights reserved.

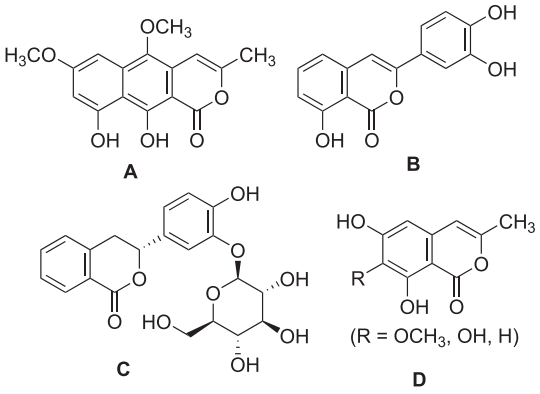

Fig. 1. Examples of isocoumarin derivatives possessing anti-inflammatory activities.

isocoumarin thunberginol (**B**, Fig. 1) showed inhibition of PGE2 production in the same study. Recently, a natural isocoumarin GDC [3R-(4′-hydroxyl-3′-O-β-D-glucopyranosyl phenyl)-dihydro isocoumarin] (**C**, Fig. 1) has shown remarkable anti-inflammatory activities including the inhibition of production of tumor necrosis factor alpha (TNF-α) and interleukin-6 (IL-6) induced by LPS [5]. Interestingly, exploration of isocoumarin derivatives as inhibitor of PDE4 (phosphodiesterase 4) is rather uncommon though inhibition of calmodulin-sensitive cyclic guanosine 3′,5′-monophosphate phosphodiesterase by three natural isocoumarins (**D**, Fig. 1) was studied way back in 1989 [6]. Notably, the inhibitors of PDE4 are not only known to be useful for the treatment of inflammatory diseases [7–9] like COPD/asthma, psoriasis, psoriatic arthritis etc but also have been suggested to attenuate the cytokine storm in COVID-19 especially TNF-α [10–12]. The currently available inhibitors such as roflumilast and apremilast though found to be potent and effective but their emetic and other side effects emphasize the necessity for the discovery and development of alternative agents. In our effort [13,14] for the identification of new inhibitors of PDE4 we explored benzo[*c*]phenanthridine derivatives that were synthesized from the isocoumarin-based key intermediates (**E**, Fig. 2) [15]. Prompted by the reported usefulness of isocoumarins as anti-inflammatory agents we examined PDE4 inhibitory potential of **E** when none of these derivatives showed significant inhibition of PDE4 *in vitro*. However, introduction of an aminosulfonyl moiety to the benzene ring at C-3 position enhanced the inhibitory properties of the resultant analogue (**F**, Fig. 2) remarkably in some cases. Indeed, the role of aminosulfonyl moiety in PDE4B inhibition was further supported by the docking study of a representative molecule **F-1** (Fig. 3, see also Fig. S-6 in suppl info) where one of the oxygen atom of the $-NHSO_2$-group formed a H-bond with the HIS450 residue. Overall, with a high binding affinity (-11.9 comparable to rolipram's -10.4) **F-1** interacted well with the PDE4B *in silico* (ID: 4MYQ) *via* (i) two H-bonds with HIS450 and TYR405, (ii)

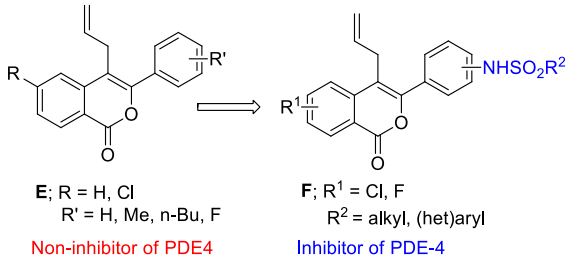

Fig. 2. Exploring isocoumarin derivatives as PDE-4 inhibitor.

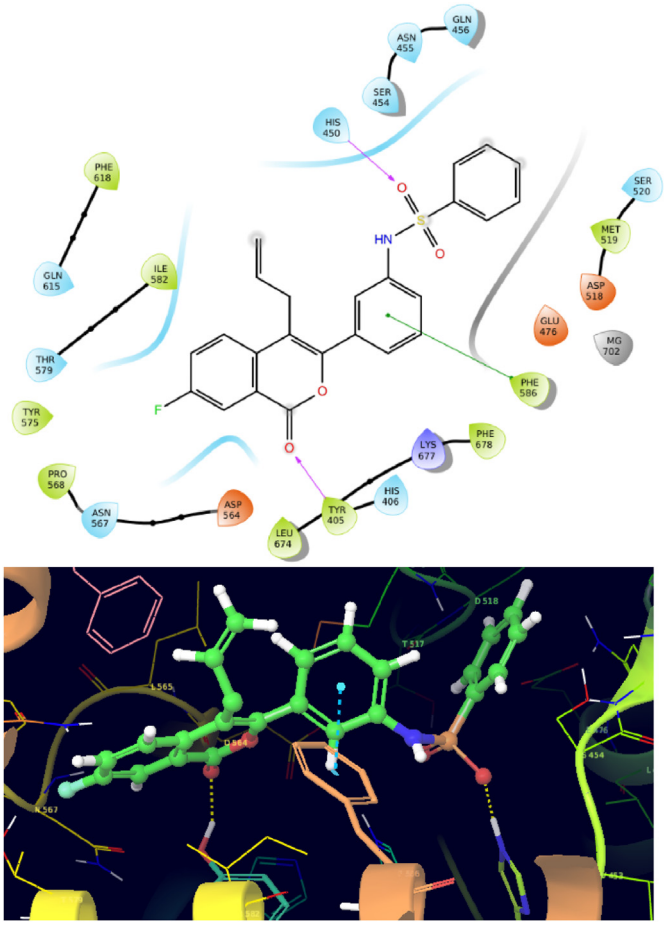

Fig. 3. 2D and 3D interaction diagram between PDE4B (ID: 4MYQ) and **F-1** (or **3q**, Table 1) prepared by using Maestro visualizer (Schrodinger, LLC) (the H-bond and pi-pi stacking are shown in magenta and green colour in 2D diagram, and yellow and cyan dashed lines in 3D diagram).

one aromatic pi interaction with PHE586 and (iii) a number of van der Waals/hydrophobic contacts with hydrophobic residues like TYR575, PHE618 etc. and hydrophobic regions of polar or charged

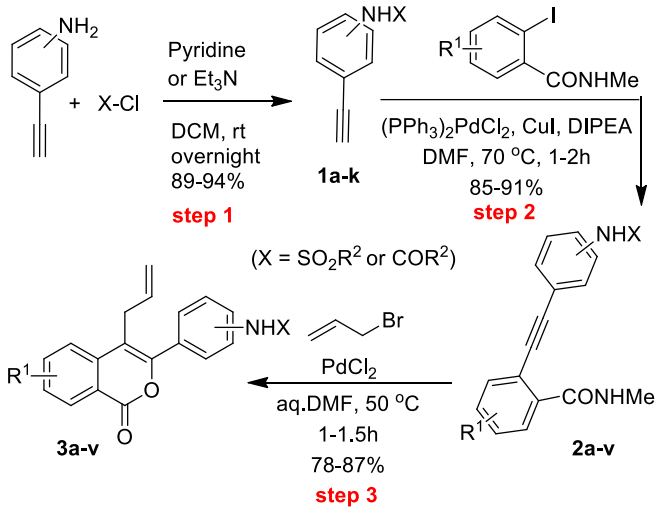

Scheme 1. Synthesis of isocoumarin derivatives containing aminosulfonyl/amino-carboxamide moiety.

Table 1
List of isocoumarin derivatives (**3**) synthesized and their *in vitro* evaluation against PDE4B.[a,b]

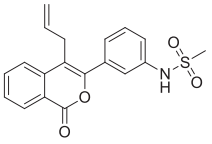

3a (82%)
PDE4B: 55.80%

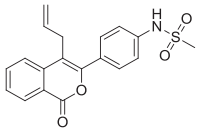

3b (80%)
PDE4B: 54.85%

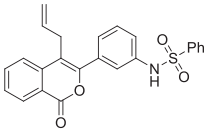

3c (84%)
PDE4B: 82.89% (IC_{50} = 1.24 ± 0.76)

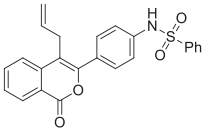

3d (81%)
PDE4B: 87.57% (IC_{50} = 3.91 ± 0.31)

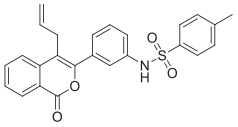

3e (86%)
PDE4B: 77.83% (IC_{50} = 2.07 ± 1.16)

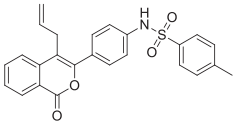

3f (82%)
PDE4B: 63.49%

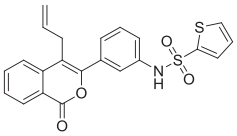

3g (85%)
PDE4B: 85.89% (IC_{50} = 1.76 ± 0.35)

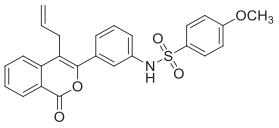

3h (80%)
PDE4B: 80.02% (IC_{50} = 3.33 ± 0.25)

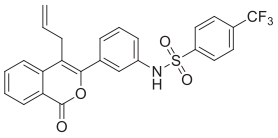

3i (78%)
PDE4B: 55.34%

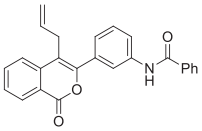

3j (82%)
PDE4B: 72.58%

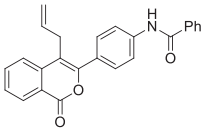

3k (79%)
PDE4B: 46.45%

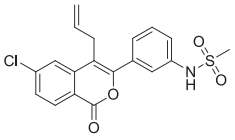

3l (83%)
PDE4B: 62.25%

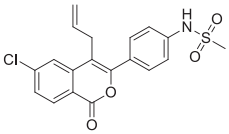

3m (80%)
PDE4B: 55.97%

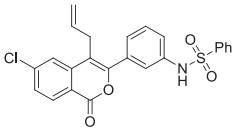

3n (84%)
PDE4B: 81.21% (IC_{50} = 4.78 ± 0.01)

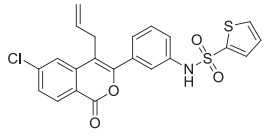

3o (82%)
PDE4B: 75.65% (IC_{50} = 4.01 ± 0.73)

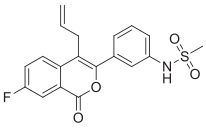

3p (85%)
PDE4B: 90.86% (IC_{50} = 1.94 ± 0.67)

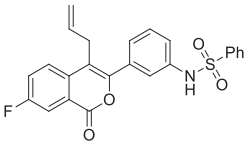

3q (86%)
PDE4B: 82.25% (IC_{50} = 0.43 ± 0.11)

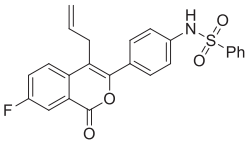

3r (79%)
PDE4B: 94.39% (IC_{50} = 1.91 ± 0.50)

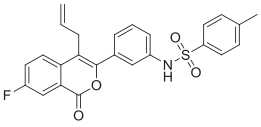

3s (83%)
PDE4B: 79.68% (IC_{50} = 3.04 ± 1.17)

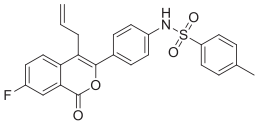

3t (80%)
PDE4B: 93.96 (IC_{50} = 2.36 ± 0.17)

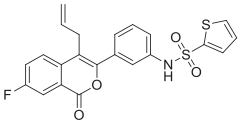

3u (87%)
PDE4B: 96.02 (IC_{50} = 0.54 ± 0.19)

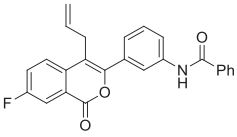

3v (80%)
PDE4B: 74.63%

[a] Figure in the bracket indicates isolated % yield.
[b] Other figures present % inhibition of PDE4B at 10 μM and IC_{50} (μM). Rolipram (PDE4B: 77.22%; IC_{50} = 0.94 ± 0.2) was used as a reference compound.

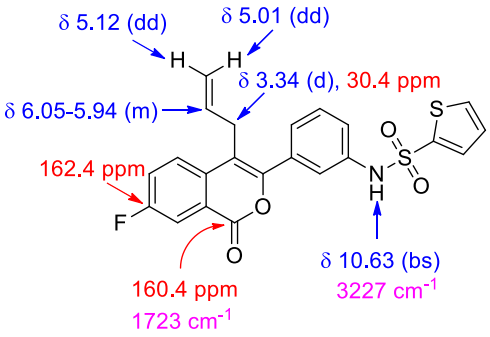

Fig. 4. Partial representation of ^{1}H as well as ^{13}C NMR and IR spectral data of compound **3u**.

residues like; SER454, ASN455, GLN456, THR579, HIS406, ASN567, GLN615 etc. Notably, in addition to participating in the hydrophobic interactions with PDE4B the allyl group enhances lipophilicity that may cause a rapid onset. Herein we present a detailed account of this study. We also examined the PDE4 inhibitory potential of the corresponding aminocarboxamide analogues designed *via* replacing the $-NHSO_2R^2$ of **F** by $-NHCOR^2$. While PDE4 inhibition of compounds containing sulphonamide moiety has been studied earlier [16,17] the synthesis and PDE4 evaluation of isocoumarin derivatives containing aminosulfonyl/aminocarboxamide moiety was not explored previously.

2. Results and discussion

2.1. Chemistry

The targeted new class of isocoumarin derivatives were synthesized *via* a Pd-catalyzed method similar to that developed by us recently (Scheme 1) [15]. This interesting approach involved the construction of a 4-allyl substituted 3-aryl isocoumarin ring starting from the appropriate 2-alkynyl benzamide derivative. Thus the commercially available terminal alkynes containing an aniline moiety were converted to the corresponding sulfonamides or amides (**1a-k**) (step-1 of Scheme 1) that on Sonogashira coupling with 2-iodobenzamides afforded a range of 2-alkynyl benzamides (**2a-v**) in good yields (step 2 of Scheme 1, see also Tables S–3 in Supp info). Treating the compound **2** with allyl bromide in the presence of $PdCl_2$ in aqueous DMF (10% H_2O in DMF) afforded the desired isocoumarins (**3a-v**) (step 3 of Scheme 1 and Table 1). Notably in compared to $Pd(OAc)_2$ used in our earlier approach [15] the relatively cheaper $PdCl_2$ was found to be more effective in the current study as the reaction was completed within 1–1.5 h (for optimization study see Tables S–5 in suppl info). Nevertheless, the starting 2-alkynyl benzamides (**2a-v**) may contain various NHX group (when X = SO_2R^2 or COR^2) and the reaction proceeded smoothly *via* C–O/C–C bond formation to give the desired products with desired regioselectivity. Indeed, the formation of no isomeric 5-membered ring product i.e. the corresponding phthalide as a side product was observed during the reaction. All the isocoumarins synthesized were characterized by spectral (NMR, MS) data. The allylic protons could be detected for most of the compounds in their ^{1}HNMR spectra generally as (i) a doublet near δ 3.3, (ii) a multiplet in the range δ 6.0-5.9 and (iii) two double doublets near δ 5.1 and 5.0 due to the CH_2, CH and $=CH_2$ moiety, respectively. The presence of lactone C=O group was indicated by the IR absorptions near 1720 cm^{-1} and the ^{13}CNMR signal near 160 ppm, respectively. The partial ^{1}H and ^{13}C NMR data along with IR absorptions of a representative compound **3u** is shown in Fig. 4. The NH and C-7 bearing a fluorine atom appeared near δ 10.6 (broad singlet) and 162 ppm in the ^{1}H and ^{13}C NMR spectra, respectively. Mechanistically [15], the reaction involved a $PdCl_2$ catalyzed 6-*endo-dig* ring closure in the presence of allyl bromide to give the isochromen-1-imine species that afforded **3** in acidic media (see Supp info).

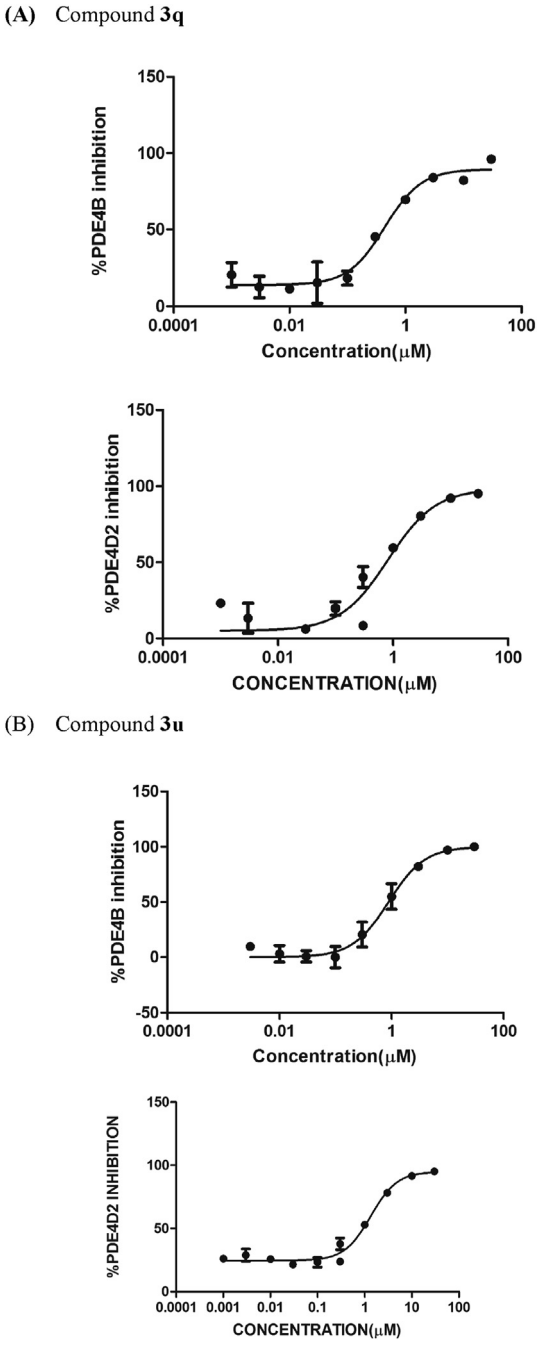

Fig. 5. Concentration dependent study of (A) compound **3q** and (B) compound **3u** against PDE4B and PDE4D.

2.2. Biology

Since PDE4B (one of the four major subtypes of PDE4 e.g. PDE4A, B, C and D) is known to be responsible for mediating LPS-induced inflammation [7–9] hence the synthesized isocoumarin derivatives were evaluated *in vitro* initially at 10 μM for their PDE4B inhibitory properties using an enzyme based assay (Table 1) [18].

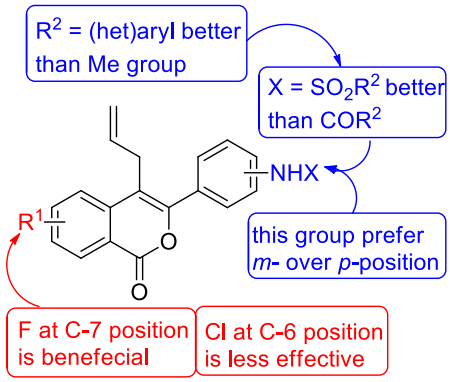

Fig. 6. Summary of SAR for PDE4B inhibitory activities of isocoumarins (**3**).

Rolipram, a well-known inhibitor of PDE4 was used as a reference compound. While most of the compounds showed mediocre to good activities the analogues that showed >75% inhibition i.e. **3c, 3d**, **3e, 3g, 3h, 3n, 3o, 3p, 3q, 3r**, **3s**, **3t** and **3u** were identified as initial hits and taken for concentration dependent studies. The IC_{50} values of these compounds are presented in Table 1 and the concentration response curves of the most active compounds **3q** and **3u** are shown in Fig. 5. Notably, while some compounds e.g. **3d**, **3r**, **3t** etc showed good inhibition initially at 10 μM their IC_{50} was found to be higher due to their inferior inhibition at low concentrations particularly below 1 μM. Though a precise Structure-Activity-Relationship (SAR) within the current series of isocoumarin derivatives was not clear it was evident that the position as well as nature of the aminosulfonyl or aminocarboxamide substituent i.e. NHX attached to the benzene ring at C-3 position of the isocoumarin ring appeared to play a key role in the PDE4 inhibitory activities (Fig. 6). In general, (i) an aminosulfonyl group was more favorable than the aminocarboxamide moiety, (ii) the NHX substituent preferred the *m*-position over the *p*-position of the C-3 benzene ring, (iii) the NHX group was preferred when X = aryl or heteroarylsulfonyl group rather than methylsulfonyl moiety (with the exception of compound **3p**), and (iv) a fluorine at the C-7 position of the isocoumarin ring was beneficial though a chlorine at C-6 position was less effective. Notably, the presence of NHX substituent at the *o*-position of the C-3 benzene ring was not assessed because this position might not be optimum for the NHX substituent to interact effectively with the target protein (due to the potential steric crowding or hindrance caused by the adjacent and proximate group or ring present within the molecule). Moreover, substituents e.g. Cl or F at C-6/C-7 but not at C-5/C-8 position of the isocoumarin ring were explored to block the potential metabolism if any under *in vivo* conditions.

While significant inhibition of PDE4D was shown by both the compound **3q** (IC_{50} = 0.90 ± 0.06 μM) and **3u** (IC_{50} = 1.34 ± 0.09 μM) (Fig. 5) the compound **3u** showed marginally better selectivity i.e. ~2.5 fold over **3q** possessing ~2 fold selectivity. Notably, while the inhibition of PDE4D was thought to be responsible for undesired side effects especially emesis later it was demonstrated that inhibition of PDE4D by allosteric inhibitors (Maximum inhibition, I_{max} 80–90%) did not cause emetic side effects [19] raising an intriguing possibility that PDE4B inhibitors with partial but not complete inhibition of PDE4D (I_{max} of ~60–80%) could be developed to treat inflammatory diseases

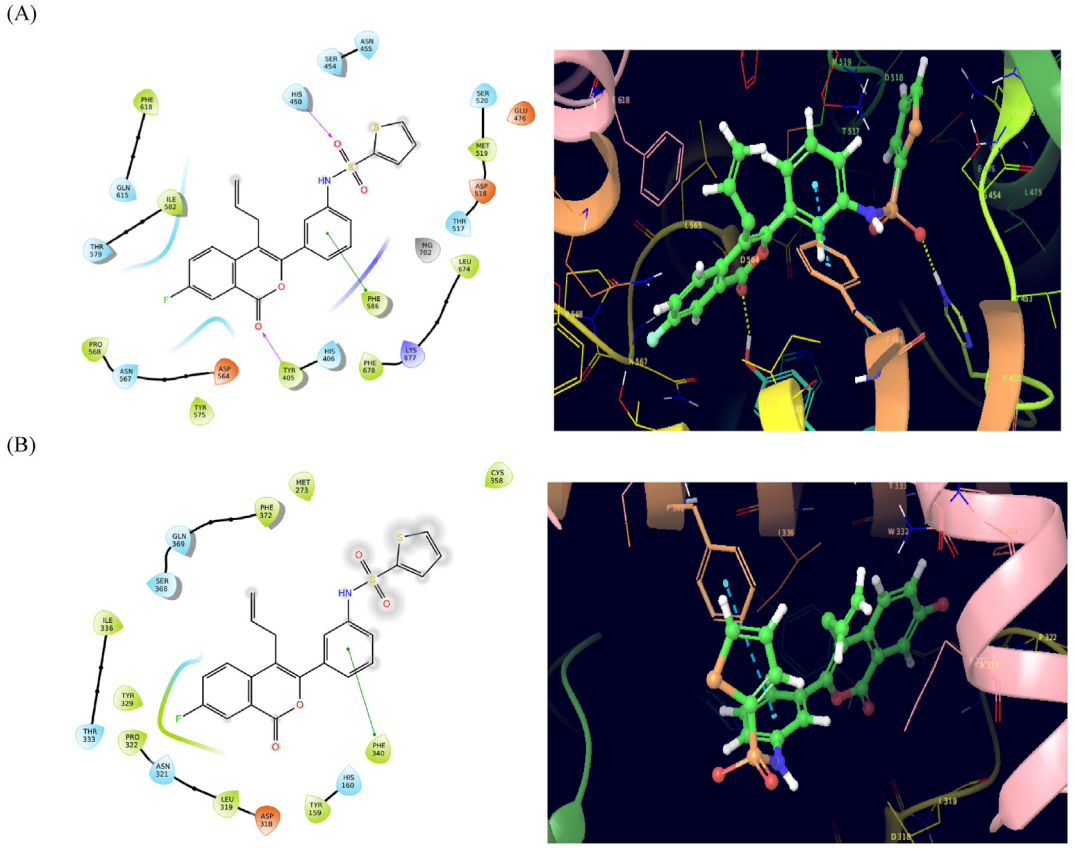

Fig. 7. (A) The 2D (H-bond in magenta and pi-pi in green colour) and 3D interaction diagram (H-bond in yellow and pi-pi stacking in cyan dashed lines) between PDE4B (ID: 4MYQ) and compound **3u**; (B) 2D and 3D interaction diagram between PDE4D (ID: 5K32) and **3u**.

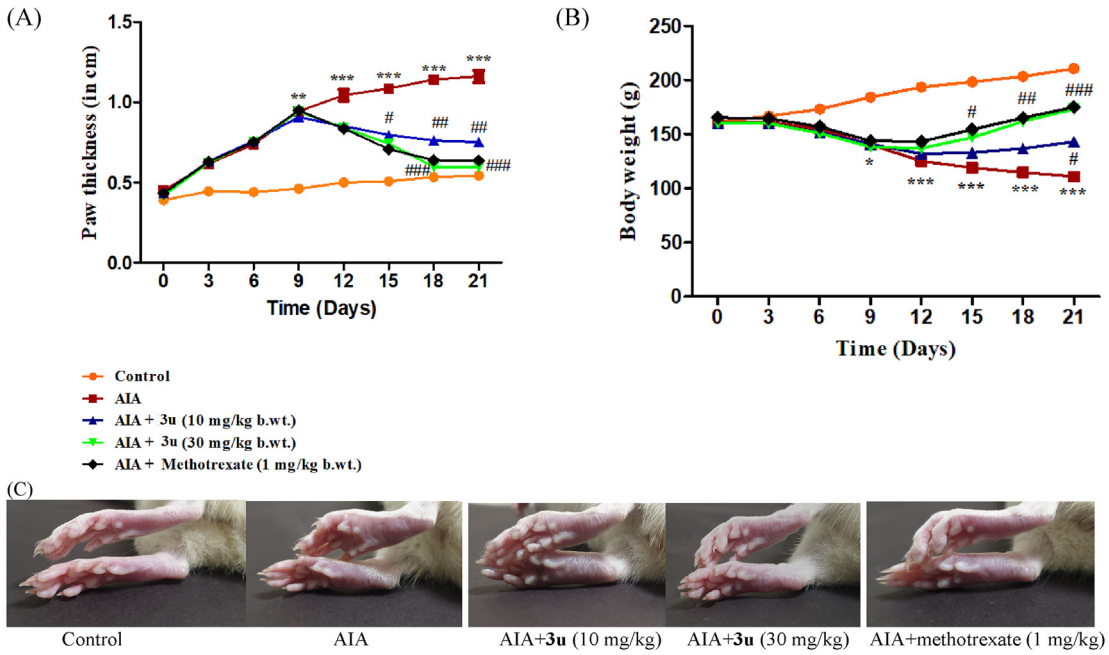

Fig. 8. Effect of compound **3u** on (A) paw swelling and (B) body weight changes in adjuvant induced arthritic (AIA rats). All error bars represent mean ± SEM. ***P < 0.001 vs control. #P < 0.05, ##P < 0.01, ###P < 0.001 vs AIA rats. (C) Macroscopic images depicting the severity of paw swelling in experimental animals on day 21.

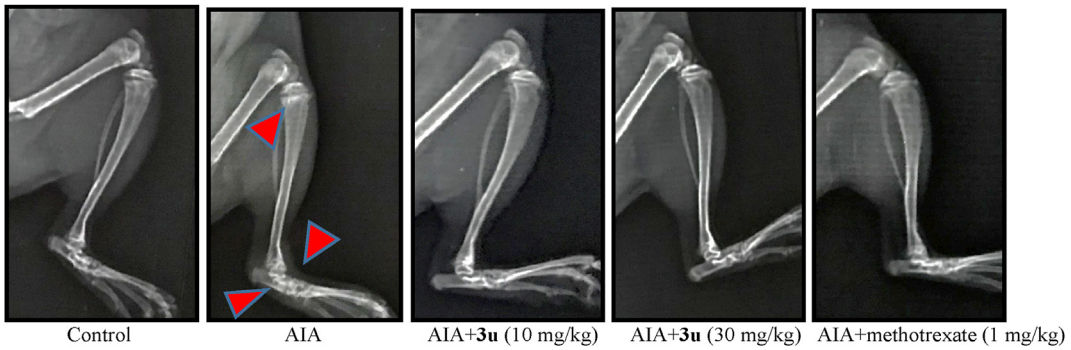

Fig. 9. Representative radiographic images of rat joints in experimental animals on day 21 (red arrow shows joint deformity).

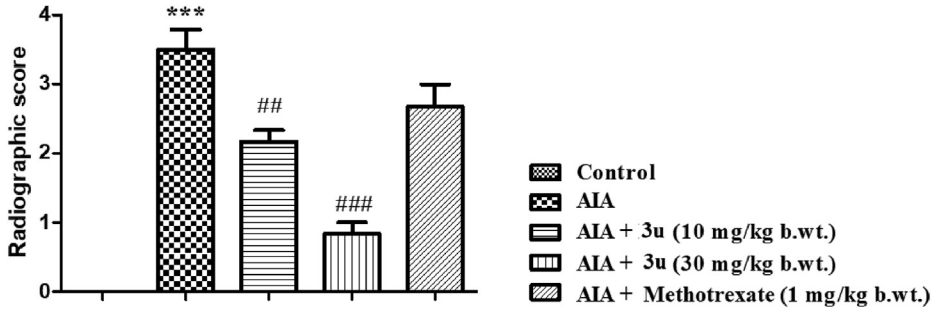

Fig. 10. Radiographic scoring graded on a semi-quantitative four-point scale of 0–4: grade 0: (absent); grade 1: (weak); grade 2: (moderate); grade 3: (high); grade 4: (very high). Radiographic scores were confirmed by independent observers on the basis of joint structural changes such as joint space, and joint deformity and averaged.

without causing emetic side effects. Thus these moderately selective isocoumarins especially **3u** seemed to be of further interest. To understand its interaction with PDE4B as well as PDE4D *in silico* the compound **3u** was docked into both the proteins (Fig. 7). The molecule participated in two H-bond interactions with HIS450 and TYR405, and one aromatic pi interaction with PHE586. Additionally, **3u** was also involved in a number of non-bonded contacts (e.g. hydrophobic/van der Waals) with hydrophobic residues ILE582, TYR575, LEU674, MET519, PRO568, PHE678 and hydrophobic regions of polar or charged residues such as ASN567, SER406 and THR579. On the other hand, **3u** showed lower number of interactions with PDE4D indicating its moderate selectivity towards

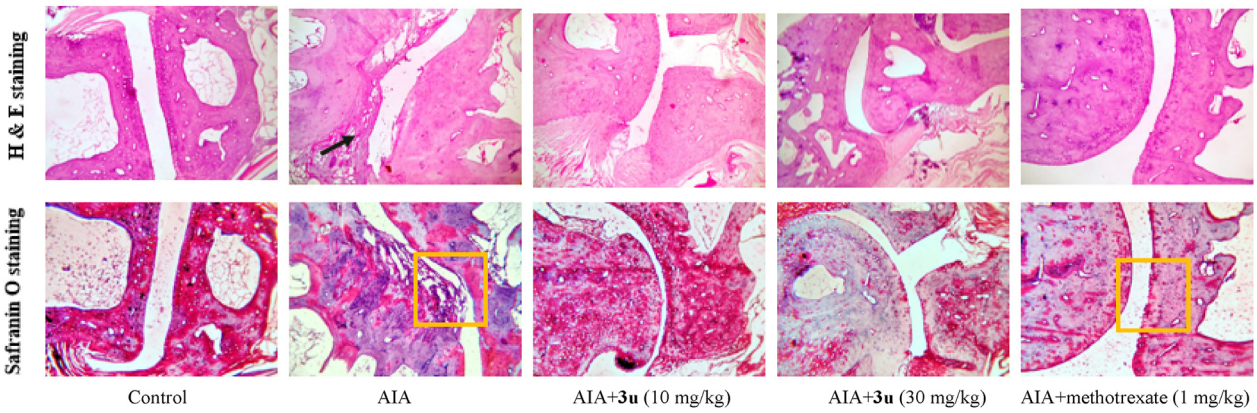

Fig. 11. Experimental rat knee joint sections were H & E stained for examining histological changes like joint space, cellular infiltration and pannus formation. Black arrow: pannus formation; yellow box: cartilage degradation (magnification: 100×).

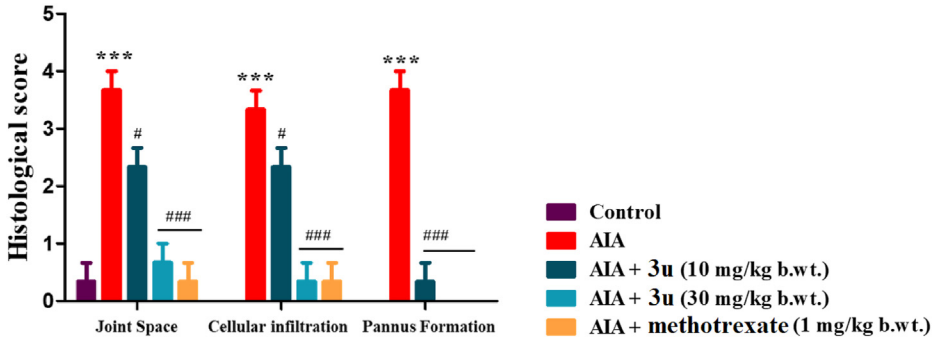

Fig. 12. Representative H & E staining scoring graded on a semi-quantitative four-point scale in a blinded manner; grade 0: (absent); grade 1: (weak); grade 2: (moderate); grade 3: (high); grade 4: (very high).

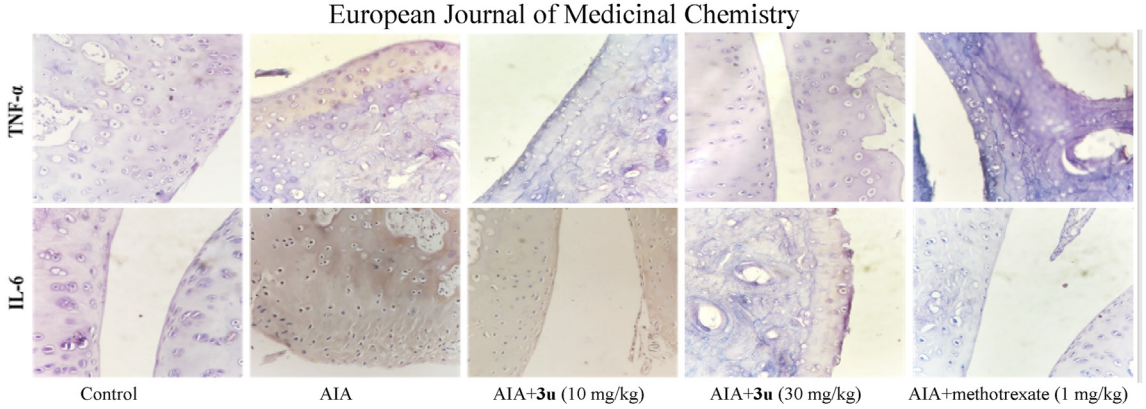

Fig. 13. Immunohistochemistry staining analysis was performed to examine for the expression of TNF-α and IL-6. (magnification: 100×).

PDE4B over D. A similar trend was observed in case of compound **3q** (or compound **F-1**) also when the molecule was docked into PDE4B (Fig. 3) as well as PDE4D (see Fig S-7, suppl info).

In a separate study the PDE4 selectivity of compound **3u** over other families of PDEs (e.g. PDE1-PDE11) was assessed using an *in vitro* enzymatic assay [14]. At 10 μM the % inhibition shown by **3u** was either low or poor, e.g. 21% (PDE1A1), 18% (PDE1B), 24% (PDE1C), 9% (PDE2A1), 11% (PDE3A), 7% (PDE3B), 8% (PDE5A1), 10% (PDE6C), 6% (PDE7A1), 3% (PDE7B), 2% (PDE8A1), 8% (PDE9A2), 12% (PDE10A1), 19% (PDE10A2) and 11% (PDE11A4) indicating its PDE4 selectivity over other PDEs.

Next, the potential for anti-inflammatory effects of compound **3u** was evaluated when the compound showed significant inhibition of TNF-α i.e. 65.5 ± 5.1, 45.6 ± 6.4, 40.3 ± 4.8 and 30.9 ± 8.3% at 10, 3, 1 and 0.3 μM, respectively (when rolipram showed 50.3 ± 1.2% inhibition at 0.1 μM). Subsequently, the therapeutic efficacy of compound **3u** was evaluated at an intraperitoneal dose of 10 and 30 mg/kg in an adjuvant induced arthritic (AIA) rat model using methotrexate (1 mg/kg) as a positive control [20]. The progression of disease severity was monitored periodically by assessing changes in body weight and paw swelling post complete Freund's adjuvant injection. As shown in Fig. 8, substantial increase in paw

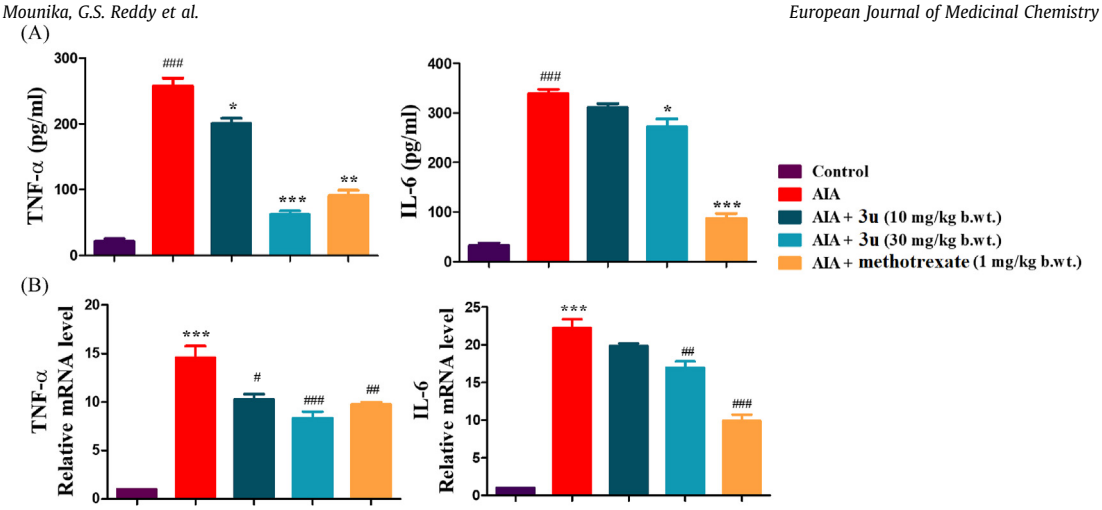

Fig. 14. Effect of 3u on the expression of pro-inflammatory molecules. (A) The expression level of TNF-α and IL-6 are examined in the serum of experimental animals. **(B)** The expression level of TNF-α and IL-6 are examined at the mRNA level in experimental animals. All error bars represent mean ± SEM. ***P < 0.001 vs control. #P < 0.05, ##P < 0.01, ###P < 0.001 vs AIA rats.

swelling and body weight loss was observed in AIA rats as compared to control rats. However, **3u** was found to be effective in reducing paw swelling in a dose dependent manner. Indeed, at 30 mg/kg the compound **3u** significantly reduced paw volume of AIA rats similar to that of 1 mg/kg of methotrexate (Fig. 8A). Similarly, **3u** (30 mg/kg) improved intestinal absorption of nutrients as observed from significant increase in body weight in AIA rats (Fig. 8B).

Histopathological examination of synovial tissues displayed joint space narrowing, abundant cellular infiltration and pannus formation in AIA rats. In addition, radiographic assessment [21] showed increased joint deformity in AIA rats (Figs. 9–13). While the methotrexate treatment was not so effective in reducing changes in joint structure deformity (perhaps due to its significant role in inflammation inhibition rather than controlling bone damage) the treatment with **3u** (30 mg/kg) decreased pathological changes and significantly reduced joint degenerative changes (Figs. 9–13). Furthermore, the expression of TNF-α and IL-6 were evaluated in the synovial tissue and serum of experimental animals. As shown in Fig. 14, an increased expression level of TNF-α and IL-6 was observed in AIA rats. However, a significant decrease in the expression level of TNF-α was observed in **3u** and methotrexate treated AIA rats as compared to AIA rats. Interestingly, not much significant changes were observed in the expression level of IL-6 upon treatment with **3u** (Fig. 14). Notably, being considered as a first line disease-modifying anti-rheumatic drug (DMARD) methotrexate is the first choice of clinicians for the treatment of rheumatoid arthritis (RA) though the drug has been shown to possess adverse effects on bone metabolism in RA patients [22]. Overall, based on the strong evidences of the anti-arthritic potential of **3u** the molecule appeared to be a promising hit and may be investigated further for its preclinical development.

In order to gain an initial assessment about potential toxicity the compound **3u** was tested against Raw 264.7 cells *via* an MTT assay [23] when the compound did not show any significant toxicity (IC_{50} > 100 μM). However, due to the presence of an allyl moiety as well 5-unsubstituted thiophene ring it was necessary to evaluate **3u** for potential toxicities *in vivo*. It is known that the allyl group not only enhance the lipophilicity but also could be the reason for potential metabolic instability to generate toxic metabolites *in vivo*. Being a toxicophore the 5-unsubstituted thiophene on the other hand is known to undergo oxidation affording hepatotoxic metabolites. Hence the compound was further evaluated for its probable toxicity specifically its potential ability to induce

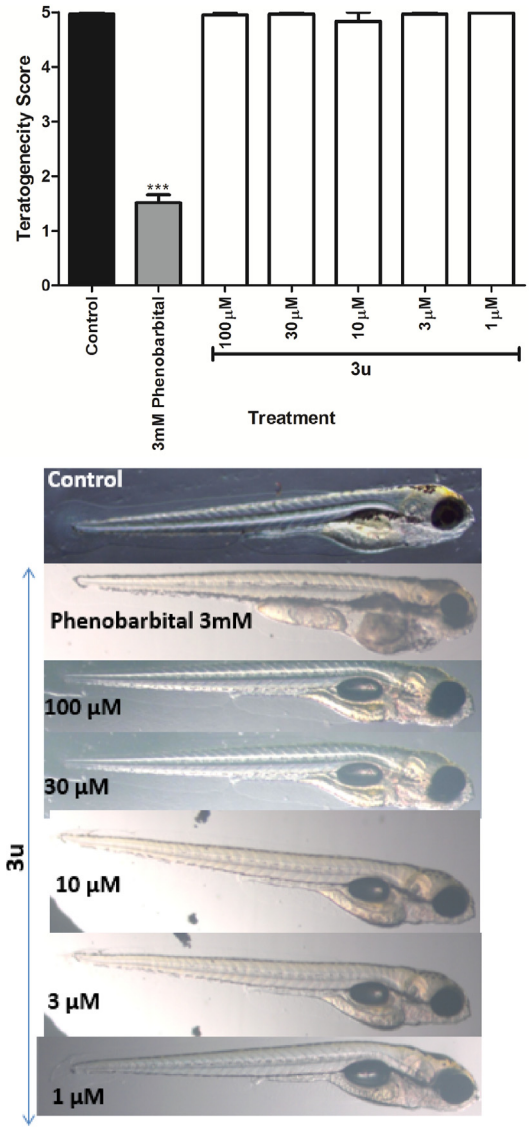

Fig. 15. Compound **3u** did not induce teratogenicity in Zebrafish embryos. Top panel: Teratogenicity scores of compound **3u** and positive control phenobarbitol. Bottom panel: Representative images of teratogenicity assay. Data are represented as mean +SEM. Statistical analysis was performed by graphpad prism software using two-way ANOVA post-hoc test. *, p < 0.05 was considered as significant.

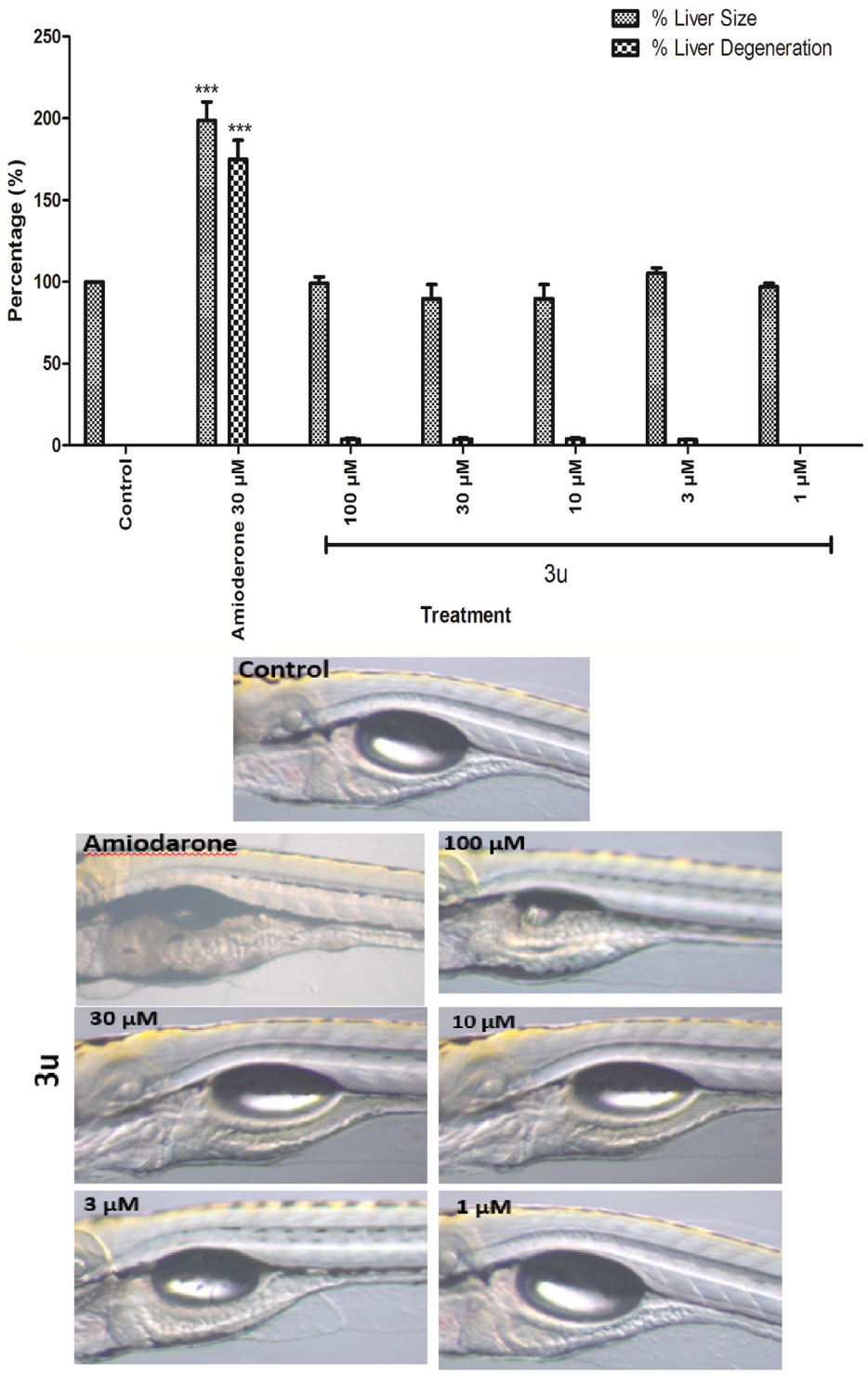

Fig. 16. Compound **3u** did not induce hepatotoxicity in Zebrafish embryos. Top panel: the graph represents the qualitative data of % liver size and % liver degeneration in compound **3u** treated embryos at different concentrations when compared to positive control amiodarone. Bottom panel: Representative images of hepatotoxicity assay. Data are represented as mean +SEM. Statistical analysis was performed by graphpad prism software using two-way ANOVA post-hoc test. ***, $p < 0.001$ was considered as significant.

teratogenicity, hepatotoxicity, cardiotoxicity and apoptosis in zebrafish. The well-known agents such as methotrexate, phenobarbitol, amiodarone, terfenadine and atrazine were used individually as a positive control in these assays respectively. Across the range of concentration tested e.g. 1, 3, 10, 30 and 100 µM the compound **3u** was found to be safe in all these toxicity assays (Figs. 15–18). Finally, we conducted some initial assessment about ADME (absorption, distribution, metabolism, and excretion) or pharmacokinetic properties of compound **3u** *in silico*. The computational ADME prediction was carried out using Swiss ADME webtool [24] and results are summarized in Table 2 (among the various descriptors only notable one are listed in the table). While the low GI absorption was predicted for **3u** an acceptable bioavailability (score 0.55) and no P-gp substrate potential was also predicted for

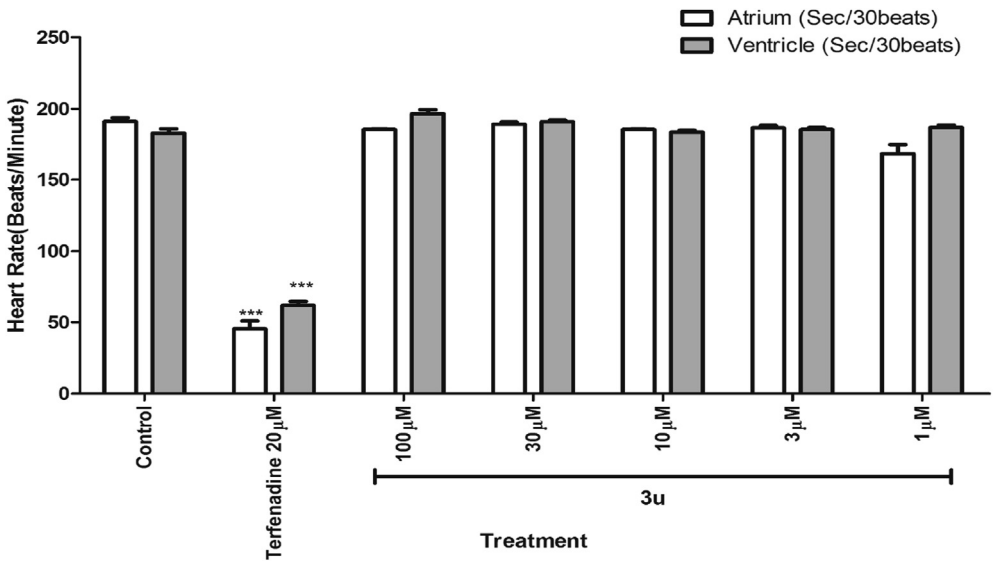

Fig. 17. Compound **3u** did not induce cardiac toxicity in Zebrafish embryos. The above graph represents the heart rate of compound **3u** treated embryos at different concentrations when compared to positive control terfenadine. Data are represented as mean ± SEM. Statistical analysis was performed by graphpad prism software using two-way ANOVA post-hoc test. ***, $p < 0.001$ was considered as significant.

this molecule. Moreover, no BBB permeation predicted for this molecule indicated its less likely interaction with the emetic center in the brain thereby avoiding the possible emetic side effects. Further, the compound **3u** did not show the violation of Lipinski or Veber rule. Overall, based on the outcome of all *in vitro* and *in vivo* studies the isocoumarin **3u** has been identified as a potential candidate that may be taken forward for further *in vivo* studies.

3. Conclusion

In view of anti-inflammatory activities of isocoumarin derivatives a new class of PDE4B inhibitors was designed *via* introducing an aminosulfonamide/aminocarboxamide moiety into the C-3 benzene ring attached to an isocoumarin framework followed by docking of a representative compound into the PDE4B *in silico*. These compounds were synthesized *via* a $PdCl_2$-catalyzed method involving the construction of a 4-allyl substituted 3-aryl isocoumarin ring starting from the appropriate 2-alkynyl benzamide derivative. The current method has some advantages over the previously reported $Pd(OAc)_2$ catalyzed method because $PdCl_2$ was cheaper and decreased the reaction time. A variety of isocoumarins were prepared in good yields and several of them showed good inhibition when evaluated initially against PDE4B *in vitro*. The SAR within the series indicated superiority of aminosulfonamide over aminocarboxamide moiety in terms of PDE4B inhibition. Two compounds **3q** and **3u** with PDE4B $IC_{50} = 0.43 \pm 0.11$ and 0.54 ± 0.19 and $\geq$ 2-fold selectivity over PDE4D emerged as initial hits. The participation of aminosulfonamide moiety in PDE4B inhibition and the reason for selectivity though moderate shown by **3q** and **3u** was analyzed by the *in silico* docking studies. In view of potential usefulness of moderately selective PDE4B inhibitors the compound **3u** (that showed PDE4 selectivity over other PDEs) was further evaluated in adjuvant induced arthritic rats. At an intraperitoneal dose of 30 mg/kg the compound showed a significant reduction in paw swelling (in a dose dependent manner), inflammation and pannus formation (in the knee joints) as well as pro-inflammatory gene expression/mRNA levels and increase in body weight along with a drastic reduction in joint degenerative changes. Moreover, besides its inhibitory activity against TNF-α and no significant toxicity in an MTT assay the compound did not show any adverse effects in a thorough toxicity (e.g. teratogenicity, hepatotoxicity, cardiotoxicity and apoptosis) studies in zebrafish. Overall, based on the outcome of all *in vitro* and *in vivo* studies the isocoumarin **3u** was identified as a new, safe and moderately selective inhibitor of PDE4B that can progress further into the pre-clinical development. Moreover, in view of the potential utility of PDE-4/TNF-α inhibitors against COVID-19 in addition to their well-known effectiveness against inflammatory diseases the current efforts on $PdCl_2$-catalyzed synthesis of a new class of isocoumarins containing aminosulfonyl/aminocarboxamide moiety towards the identification of PDE4 inhibitors may attract considerable interest.

4. Experimental section

4.1. General procedure for the preparation of compound *1*

Preparation of compound **1a-i**: Appropriate Sulfonyl chloride (1.2 mmol) was added to a solution containing 3-ethynylaniline or 4-ethynylaniline (1.0 mmol), and pyridine (3.0 mmol) in DCM (10 mL) under a nitrogen atmosphere at 0 °C for 10 min. The resulting mixture was stirred at room temperature for overnight. After completion of the reaction (indicated by TLC) DCM was evaporated. The residue was treated with 2 N aqueous HCl (10 mL) and the mixture was diluted with ice-water (60 mL) and extracted with ethyl acetate (3 x 15 mL). The organic layers were collected, combined, dried over anhydrous Na_2SO_4, filtered and concentrated under low vacuum. The residue was purified by column chromatography using hexane and EtOAc (9:1) as eluent to afford the title compound.

4.1.1. Preparation of compound *1j-k*

Appropriate benzoyl chloride (1.2 mmol) was added to a solution containing 3-ethynylaniline [or 4-ethynylaniline (1.0 mmol)], and triethylamine (3.0 mmol) in DCM (10 mL) under a nitrogen atmosphere at 0 °C for a duration of 10 min. The resulting mixture was stirred at room temperature for overnight. After completion of the reaction (indicated by TLC) DCM was evaporated. The mixture was diluted with cold water (60 mL) and extracted with ethyl

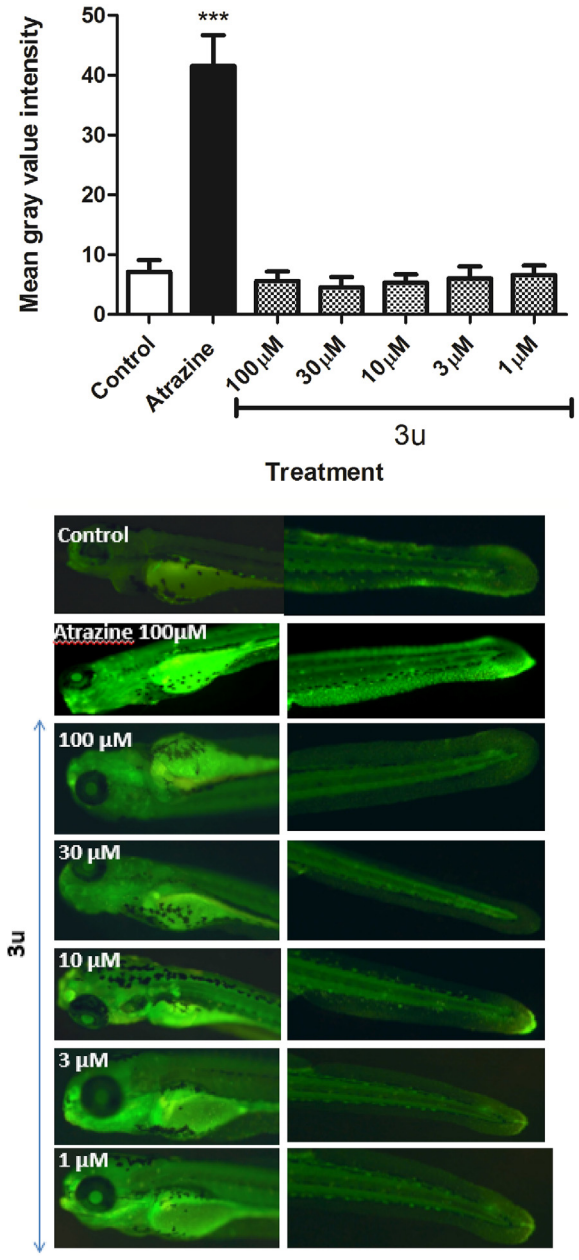

Fig. 18. Compound **3u** did not induce apoptosis in Zebrafish embryos. Top panel: the graph represents the apoptosis intensity (mean grey value intensity) of compound **3u** treated embryos at different concentrations and compared to the positive control atrazine. Bottom panel: Representative images of apoptosis induction assay. Data are represented as mean ± SEM. Statistical analysis was performed by graphpad prism software using two-way ANOVA post-hoc test. ***, $p < 0.001$ was considered as significant.

acetate (3 x 15 mL). The organic layers were collected, combined, dried over anhydrous Na_2SO_4, filtered and concentrated under low vacuum. The residue was purified by column chromatography using 9:1 hexane-EtOAc as eluent to afford the title compound.

4.2. General procedure for the preparation of compound *2*

Aryl acetylenes (**1**) (1.2 mmol) was added to a solution of 2-iodo-*N*-methylbenzamide [or substituted 2-iodo-*N*-methylbenzamide (1.0 mmol)], $(PPh_3)_2PdCl_2$ (5 mol%), CuI (5 mol%) and *N*,*N*-Diisopropylethylamine (3.0 mmol) in DMF (10 mL) under a nitrogen atmosphere. The mixture was stirred at 70 °C for 1–2 h. After completion of the reaction (confirmed by TLC), the mixture was diluted with cold water (60 mL) and extracted with ethyl acetate (3 x 15 mL). The organic layers were collected, combined, dried over anhydrous Na_2SO_4, filtered, and concentrated under low vacuum. The residue was purified by column chromatography using hexane and EtOAc (7:3) as eluent to afford the title compound.

Table 2
Computational ADME prediction of **3u**.

Properties	Molecule 3u
(i) Physicochemical	
Molecular Weight (g/mol)	441.50
Consensus Log P[a]	4.74
Log S (ESOL)[b]	−5.72 (moderately soluble)
(ii) Pharmacokinetics	
GI[c] absorption	Low
P-gp[d] substrate	No
BBB[e] permeation	No
(iii) Druglikenss	
Lipinski rule	No violation
Veber rule	No violation
Bioavailability score	0.55

[a] Log P: Lipophilicity.
[b] Log S (ESOL): water solubility, calculated by ESOL method which is a Quantitative Structure-Property Relationship (QSPR) based model.
[c] GI: Gastrointestinal.
[d] P-gp: permeability glycoprotein.
[e] BBB: Blood Brain Barrier.

4.3. General procedure for the preparation of compound *3*

To a solution of compound **2** (1.0 mmol) and $PdCl_2$ (5 mol%) in 9:1 DMF: H_2O (5 mL) was added allyl bromide (1.5 mmol) under a nitrogen atmosphere. The mixture was stirred at 50 °C for 1–1.5 h. After completion of the reaction (indicated by TLC), the mixture was diluted with ice-water (60 mL) and extracted with ethyl acetate (3 x 15 mL). The organic layers were collected, combined, dried over anhydrous Na_2SO_4, filtered, and concentrated under low vacuum. The residue was purified by column chromatography using 9:1 hexane-EtOAc as eluent to afford the title compound **3**.

Physical and spectroscopic characterization data of all the synthesized compounds are given in the supplementary data.

Declaration of competing interest

The authors declare that they have no known competing financial interests or personal relationships that could have appeared to influence the work reported in this paper.

Acknowledgements

Authors acknowledge the financial support received from Department of Biotechnology, New Delhi, India (Grant No. BT/PR22126/BRB/10/1585/2017). Authors thank the Management of DRILS, Hyderabad, India, and Manipal University, Manipal, India for encouragement and support.

Appendix A. Supplementary data

Supplementary data to this article can be found online at https://doi.org/10.1016/j.ejmech.2021.113514.

References

[1] S. Pal, M. Pal, Isocoumarin, Thiaisocoumarin and Phosphaisocoumarin: Natural Occurrences, Synthetic Approaches and Pharmaceutical Applications, Elsevier, Paperback, 2018, ISBN 9780128154113.

[2] L.C. Di Stasi, D. Camuesco, A. Nieto, W. Vilegas, A. Zarzuelo, J. Galvez, Intestinal anti-inflammatory activity of paepalantine, an isocoumarin isolated from the capitula of Paepalanthus bromelioides, in the trinitrobenzenesulphonic acid model of rat colitis, Planta Med. 70 (2004) 315–320.

[3] G. Qadeer, N.H. Rama, M. Gardu~no-Ramírez, Synthesis and anti-inflammatory activity of fluorinated isocoumarins and 3, 4-dihydroisocoumarins, J. Fluor. Chem. 128 (2007) 641–646.

[4] M. Ramanan, S. Sinha, K. Sudarshan, I.S. Aidhen, M. Doble, Inhibition of the enzymes in the leukotriene and prostaglandin pathways in inflammation by 3-aryl isocoumarins, Eur. J. Med. Chem. 124 (2016) 428–434.

[5] Y. Zhang, G. Yan, C. Sun, L. Nan, X. Wang, W. Xu, K. Chu, Compound GDC, an isocoumarin glycoside, protects against LPS-induced inflammation and potential mechanisms *in vitro*, Inflammation 42 (2019) 506–515, https://doi.org/10.1007/s10753-018-0908-2.

[6] V.R. Hegde, H. Wittreich, M.G. Pate, A.C. Horan, R.F. Hart, J.J. Troyanovich, M.S. Puar, V.P. Gullo, Naturally produced isocoumarins: inhibitors of calmodulinsensitive cyclic guanosine 3',5'-monophosphate phosphodiesterase, J. Ind. Microbiol. 4 (1989) 209–214.

[7] H. Li, J. Zuo, W. Tang, Phosphodiesterase-4 inhibitors for the treatment of inflammatory diseases, Front. Pharmacol. 9 (2018) 1048, https://doi.org/10.3389/fphar.2018.01048.

[8] C.H. Lin, S.H. Chang, J.Y. Fang, Recent advances using phosphodiesterase 4 (PDE4) inhibitors to treat inflammatory disorders: animal and clinical studies, Curr. Drug Ther. 11 (2016) 21–40.

[9] A. Kodimuthali, S.S.L. Jabaris, M. Pal, Recent advances of phosphodiesterase 4 inhibitors for the treatment of asthma and chronic obstructive pulmonary disease, J. Med. Chem. 18 (2008) 5471–5489.

[10] C. Bridgewood, G. Damiani, K. Sharif, A. Watad, N.L. Bragazzi, L. Quartuccio, S. Savic, D. McGonagle, Rationale for evaluating PDE4 inhibition for mitigating against severe inflammation in COVID-19 pneumonia and beyond, Isr. Med. Assoc. J. 22 (2020) 335–339.

[11] M. Dalamaga, I. Karampela, C.S. Mantzoros, Commentary: phosphodiesterase 4 inhibitors as potential adjunct treatment targeting the cytokine storm in COVID-19, Metab. Clin. Exp. 109 (2020), 154282.

[12] R. Chemboli, R. Kapavarapu, K. Deepti, K.R.S. Prasad, A.G. Reddy, A.V.D.N. Kumar, M.V.B. Rao, M. Pal, Pyrrolo[2,3 -b]quinoxalines in attenuating cytokine storm in COVID-19: their sonochemical synthesis and *in silico*/*in vitro* assessment, J. Mol. Struct. 1230 (2021), 129868.

[13] D.R. Gorja, S. Mukherjee, C.L.T. Meda, G.S. Deora, K.L. Kumar, A. Jain, G.H. Chaudhari, K.S. Chennubhotla, R.K. Banote, P. Kulkarni, K.V.L. Parsa, K. Mukkanti, M. Pal, Novel N-indolylmethyl substituted olanzapine derivatives: their design, synthesis and evaluation as PDE4B inhibitors, Org. Biomol. Chem. 11 (2013) 2075–2079.

[14] R. Sunke, R. Bankala, B. Thirupataiah, E.V.V.S. Ramarao, J.S. Kumar, H.M. Doss, R. Medishetti, P. Kulkarni, R.K. Kapavarapu, M. Rasool, J. Mudgal, J.E. Mathew, G.G. Shenoy, K.V.L. Parsa, M. Pal, $InCl_3$ mediated heteroarylation of indoles and their derivatization *via* C-H activation strategy: discovery of 2-(1Hindol-3-yl)-quinoxaline derivatives as a new class of PDE4B selective inhibitors for arthritis and/or multiple sclerosis, Eur. J. Med. Chem. 174 (2019) 198–215.

[15] B. Thirupataiaha, G.S. Reddy, S.S. Ghule, J.S. Kumar, G. Mounika, K.A. Hossain, J. Mudgal, J.E. Mathew, G.G. Shenoy, K.V.L. Parsaa, M. Pal, Synthesis of 11,12-dihydro benzo[c]phenanthridines *via* a Pd-catalyzed unusual construction of isocoumarin ring/$FeCl_3$-mediated intramolecular arene-allyl cyclization: first identification of a benzo[c]phenanthridine based PDE4 inhibitor, Bioorg. Chem. 97 (2020), 103691.

[16] S.V. Reddy, G.M. Rao, B.V. Kumar, C.L.T. Meda, G.S. Deora, K.S. Kumar, K.V.L. Parsa, M. Pal, Novel imidazophenoxazine-4-sulfonamides: their synthesis and evaluation as potential inhibitors of PDE4, Bioorg. Med. Chem. 21 (2013) 1952–1963, https://doi.org/10.1016/j.bmc.2013.01.023.

[17] J.G. Montana, G.M. Buckley, N. Cooper, H.J. Dyke, L. Gowers, J.P. Gregory, P.G. Hellewell, H.J. Kendall, C. Lowe, R. Maxey, J. Miotla, R.J. Naylor, K.A. Runcie, B. Tuladhar, J.B. Warneck, Aryl sulfonamides as selective PDE4 inhibitors, Bioorg. Med. Chem. Lett 8 (1998) 2635–2640, https://doi.org/10.1016/s0960-894x(98)00491-0.

[18] P. Wang, J.G. Myers, P. Wu, B. Cheewatrakoolpong, R.W. Egan, M.M. Billah, Expression, purification, and characterization of human cAMP-specific phosphodiesterase (PDE4) sub-types A, B, C, and D, Biochem. Biophys. Res. Commun. 234 (1997) 320–324.

[19] A.B. Burgin, O.T. Magnusson, J. Singh, P. Witte, B.L. Staker, J.M. Bjornsson, M. Thorsteinsdottir, S. Hrafnsdottir, T. Hagen, A.S. Kiselyov, L.J. Stewart, M.E. Gurney, Design of phosphodiesterase 4D (PDE4D) allosteric modulators for enhancing cognition with improved safety, Nat. Biotechnol. 28 (2010) 63–70, https://doi.org/10.1038/nbt.1598.

[20] A. Koyama, A. Tanaka, H. To, Daily oral administration of low-dose methotrexate has greater antirheumatic effects in collagen-induced arthritis rats, J. Pharm. Pharmacol. 69 (2017) 1145–1154.

[21] R. Ganesan, H.M. Doss, M. Rasool, Majoon ushba, a polyherbal compound ameliorates rheumatoid arthritis *via* regulating inflammatory and bone remodeling markers in rats, Cytokine 77 (2016) 115–126.

[22] J. Świerkot, K. Gruszecka, A. Matuszewska, P. Wiland, Assessment of the effect of methotrexate therapy on bone metabolism in patients with rheumatoid arthritis, Arch. Immunol. Ther. Exp. 63 (2015) 397–404.

[23] T. Mosmann, Rapid colorimetric assay for cellular growth and survival: application to proliferation and cytotoxicity assays, J. Immunol. 65 (1983) 55–63.

[24] A. Daina, O. Michielin, V. Zoete, SwissADME: a free web tool to evaluate pharmacokinetics, drug-likeness and medicinal chemistry friendliness of small molecules, Sci. Rep. 7 (2017) 1–13.